REPORT 1261

THE NEAR NOISE FIELD OF STATIC JETS AND SOME MODEL STUDIES OF DEVICES FOR NOISE REDUCTION [1]

By Leslie W. Lassiter and Harvey H. Hubbard

SUMMARY

Experimental studies of the pressure fluctuations near jet exhaust streams were made during unchoked operation of a turbojet engine and a 1-inch-diameter high-temperature model jet and during choked operation of various sizes of model jets with unheated air. The tests for unchoked operation indicate a random spectrum of rather narrow band width which varies in frequency content with axial position along the jet. Pressure surveys from the model tests along lines parallel to the 15° jet boundary indicate that the station of greatest pressure fluctuations is determined by the jet velocity and the radial distance, with a tendency of the maximum to shift downstream as either parameter is increased. From model tests the magnitude of the fluctuations appears to increase as about the second power of jet velocity at points just outside the jet boundary and as increasingly higher powers of jet velocity as distance from the boundary is increased. A laboratory method of noise reduction with model jets was found to produce large decreases in the magnitude of the lower-frequency components of the spectra and thereby also to reduce the total radiated energy.

Choked operation of model jets with unheated air indicates the appearance of a discrete-frequency component of very large magnitude. Shadowgraph records of the flow show that this condition is associated with the appearance of flow formations suggestive of partly formed toroidal vortices in the vicinity of the shocks. Elimination of these formations is found to eliminate the discrete component and thereby to reduce the overall noise level.

INTRODUCTION

It is well known that the turbojet is a generator of intense pressure fluctuations. In view of this fact, it is important that the designer and operator of turbojet-powered aircraft be able to predict the nature and severity of these fluctuations both in the vicinity of the engine (the near field) and at large distances from it (the far field).

The far-field aspect of the problem is of concern to a great number of people, including airport workers as well as the general public, and appreciable research, both theoretical and experimental, has been done on that phase of the problem. For example, reference 1 presents the results of an experimental evaluation from model jets of the effects of various geometric and flow parameters and compares model and full-scale pressure fields, while a detailed survey of the pressure field of a full-scale configuration is given in reference 2. In reference 3 it has been shown that the problem is subject to qualitative analytical treatment for distances that are large relative to the radiated wavelengths.

Of the investigations reported to date, only that of reference 4 has dealt with the pressure fluctuations in the immediate vicinity of the jet (the near field), and it is in this region that some of the more serious problems arise. Service crews and test-stand personnel work regularly in the extremely high pressure levels of the near field. Occupants of the aircraft are, in a sense, in the near field also. Thus, from consideration of personal discomfort a smaller group is affected but to a much larger extent than the general public. Structural problems arise in the near field also. In several instances structural members of the aircraft have developed fatigue failures from the oscillatory loads imposed by pressure fluctuations from the engine. Generally, these failures have been in secondary members but, with more powerful engines, the possibility that the primary tail structure of some multiengine configurations may be affected must be considered. Structural problems may also arise in the operation of ground mufflers which enclose the jet tailpipe with only small clearances between the cell walls and the jet stream. The purpose of the present investigation is therefore to make a systematic study of the near pressure field of both unchoked and choked jets. In discussion of unchoked operation, data from the survey of a full-scale engine are used primarily, although some data from high-temperature model jets are included to indicate probable trends and to clarify some of the full-scale results. Since an extensive range of overpressure is not generally available in static operation of turbojets, the characteristics of choked operation were explored with model jets only.

In order to avoid ambiguity of nomenclature, some explanation of the usage of the present report appears warranted. The terms "noise" and "sound pressure" are used interchangeably in discussion of the near-field pressure fluctuations. However, it is recognized that, because the measurements were made in the near field where sound pressure and particle velocity are not in phase, the data are in many cases not indicative of the radiated sound energy.

[1] Supersedes NACA Technical Note 3187 by Leslie W. Lassiter and Harvey H. Hubbard, 1954.

The choice of words is therefore primarily one of convenience.

SYMBOLS

$\overline{p}$	overall pressure flucutations, lb/sq ft
x	distance along flow axis, in.
Δx	distance between shocks, in.
y	distance from longitudinal axis of jet, in.
z	distance from center of nozzle or orifice to observer, in.
d	radial distance from 15° boundary, in.
D	nozzle or orifice diameter, in.
D_a	diameter of auxiliary orifice
U	jet velocity, fps
T	jet-fluid temperature, °F
p	pressure, lb/sq in.
p_s/p_0	nozzle pressure ratio
f	frequency, cps or kcps
λ	wavelength, in.
ψ	azimuth angle (zero or jet axis in front), deg

Subscripts:

e	condition at jet exit
s	initial chamber condition (stagnation)
a	auxiliary
0	ambient-air conditions

APPARATUS AND METHODS

Tests were conducted with a full-scale turbojet engine and with various model nozzles and orifices of from 0.275 inch to 2.00 inches in diameter for the purpose of determining the characteristics of the near pressure field associated with their operation. The full-scale measurements were made during ground runs of a J–33–A–17a engine having a tailpipe diameter of 18⅜ inches and with a rated thrust of 3,825 pounds. The engine was installed in an operational fighter airplane, which was positioned on a paved taxi strip approximately 300 feet from any large reflecting surfaces other than the ground. The tailpipe center line was about 36 inches above ground level and parallel to it.

The model configurations were tested while fitted to the end of the settling chamber shown schematically in figure 1. The chamber had an inside diameter of 6.00 inches and a length of 6 feet and was supplied with air from a storage tank at a pressure of 100 lb/sq in. A large part of the chamber length was filled with a cylinder of porous, rubberized material for the purpose of minimizing extraneous noise generated inside the chamber and at the control valve.

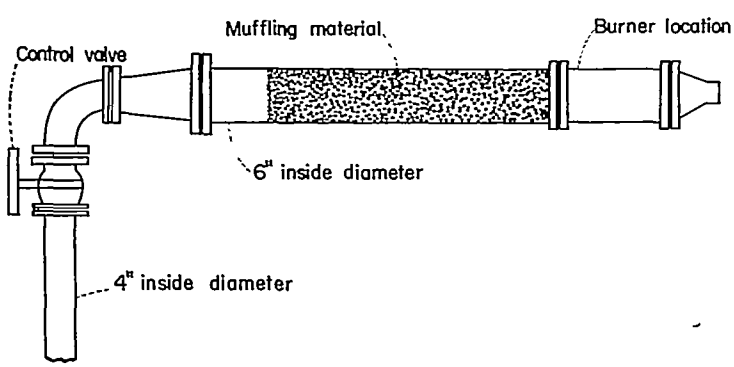

FIGURE 1.—Schematic layout of model test configuration.

This arrangement permitted measurements to be made at velocities as low as 100 fps without the appearance in the spectrum of extraneous components of any consequence.

During a part of the tests it was desired to operate the model at a temperature of the order of that in a turbojet. For this purpose, an acetylene burner of the ring type was installed in the settling chamber just downstream of the sound-absorbing material with an asbestos gasket inserted between the two chamber sections. With this arrangement, temperatures up to 1,800° were readily obtained. Operation of the burner was generally limited to the unchoked-nozzle condition. All measurements during choked operation were made with unheated air; however, enough choked operation with heated air was employed to verify the existence of the phenomena observed with unheated air.

The instrumentation used is illustrated schematically in figure 2 (a). Pressure fluctuations were detected with two sound-pressure-measurement systems. The first of these, and the one ordinarily used, has essentially a flat frequency response from 20 to 20,000 cps and cuts off at 15 and 38,000 cps. The second system, which was used only to monitor the first, has a response which is flat up to 100,000 cps. Output of the sound-measuring system was channeled to a cathode-ray oscillograph for waveform observation, an electronic voltmeter for overall pressure determination, and a Panoramic Sonic Analyzer for spectrum studies. The Panoramic is a variable-band-width instrument, the band width varying from 50 cps at 100 cps to 550 cps at 10,000 cps; thus it will not yield the true spectrum shape without correction, as will a constant-band-width analyzer. However, comparison of a few representative spectra from the Panoramic analyzer and from a constant-band-width analyzer indicated that for the qualitative purposes of this report the uncorrected Panoramic analysis is satisfactory.

Figure 2 (b) illustrates schematically the instrumentation used for motion studies of the shock formations during choked operation. The gas-discharge point-source light and the high-speed camera constitute a simple shadowgraph. Between these components is inserted a light baffle (oriented parallel to the jet axis) which allows only a fine line of light to reach the camera. The shock-wave segment being viewed then appears as a point of different intensity in that line, and a time history of its axial motion is obtained as the film moves.

More detailed studies of the flow during choked operation were made with a conventional shadowgraph system, the design of which was essentially a duplication of that described in reference 5. The light system consisted of a 15,000-volt power supply used to charge a 0.125-microfarad condenser, a gate circuit for firing control, and an arc unit. The arc unit confined the discharge to a very small volume and produced an extremely intense light flash of short duration. The light source was effectively of only ¼-inch diameter and thus afforded excellent resolution in the photographs.

RESULTS AND DISCUSSION

Surveys of the near pressure field were made during choked operation of a turbojet engine and during both unchoked and choked operation of model jet configurations. Unless otherwise indicated all unchoked model data were

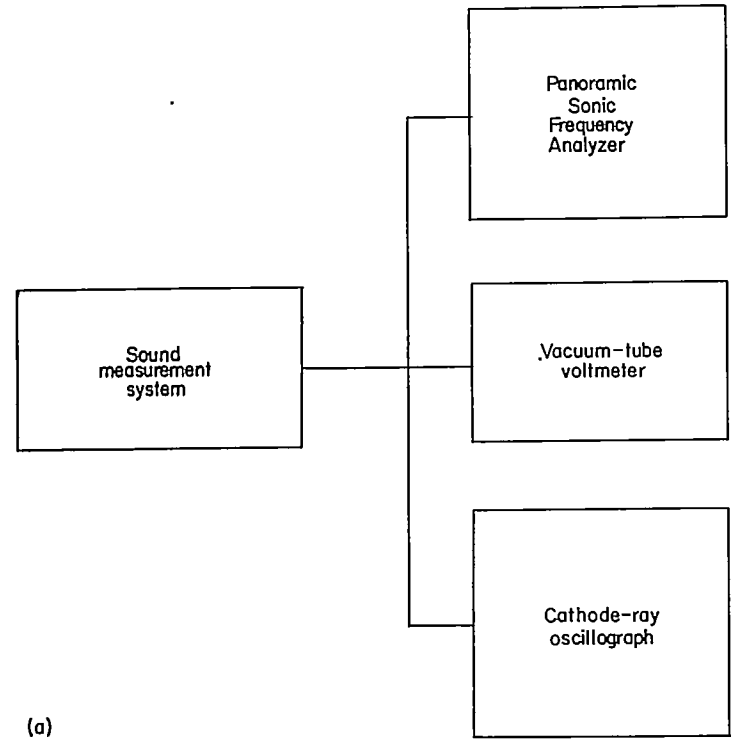

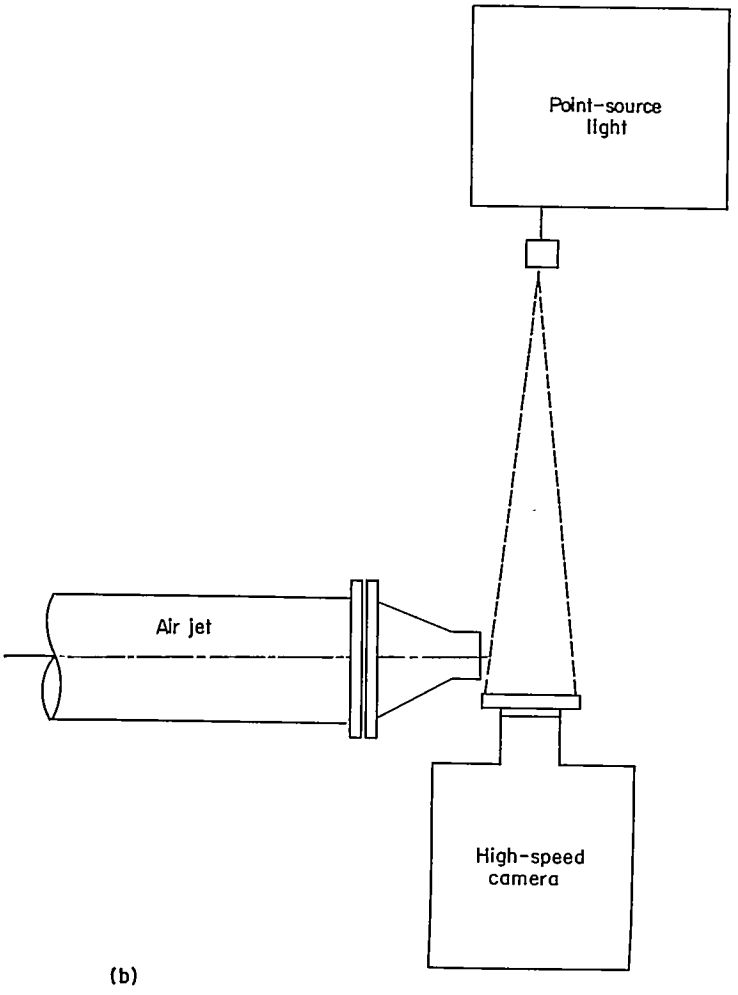

(a) Electronic instrumentation.
(b) Photographic equipment.

FIGURE 2.—Schematic diagram of instrumentation used in tests.

obtained with heated air; whereas the entire choked survey was made with unheated air. The pressure measurements were made at various axial and radial positions near the jet boundary.

UNCHOKED OPERATION OF TURBOJET ENGINE

Frequency content.—The frequency spectrum of pressure fluctuations generated by subsonic flow from the turbojet is ordinarily continuous; that is, it contains all frequencies within a given band. In the proximity of the jet boundary the frequency band may become very narrow and its limits may vary with the point of observation along the boundary. A sample spectrum, obtained at a point 2 diameters from the boundary and 15 diameters downstream of the turbojet tailpipe, is shown in figure 3. This sample is a logarithmic plot of pressure fluctuation as a function of frequency, obtained by photographing the screen of the frequency analyzer during 15 consecutive trace sweeps. It illustrates the continuous nature of the frequency content and, by the vertical spread of successive traces, the randomness of amplitude also. Evident, too, is the fact that the more important pressure fluctuations occur within a rather narrow frequency band, which at this particular position is centered at about 0.1 kcps. At points nearer the nozzle the predominant components are of considerably higher frequency (600 to 1,000 cps at the nozzle) and the band tends to become broader.

Magnitude of pressure fluctuations.—The effects of axial and radial distance on the magnitude of the pressure fluctuations for the turbojet engine operating at rated thrust are given in figure 4. Figure 4 (a) illustrates the distribution of pressure in two arbitrary frequency bands along a line parallel to the 15° jet boundary and 2 nozzle diameters from the boundary. The two bands, 15 cps to 150 cps and 150 cps to 15,000 cps, were selected purely as a matter of convenience; however, the lower band may be of particular interest inasmuch as some important structural resonances occur in that range. In the higher frequency distribution, a maximum is indicated at a point 1 nozzle diameter downstream; however, the spectrum records

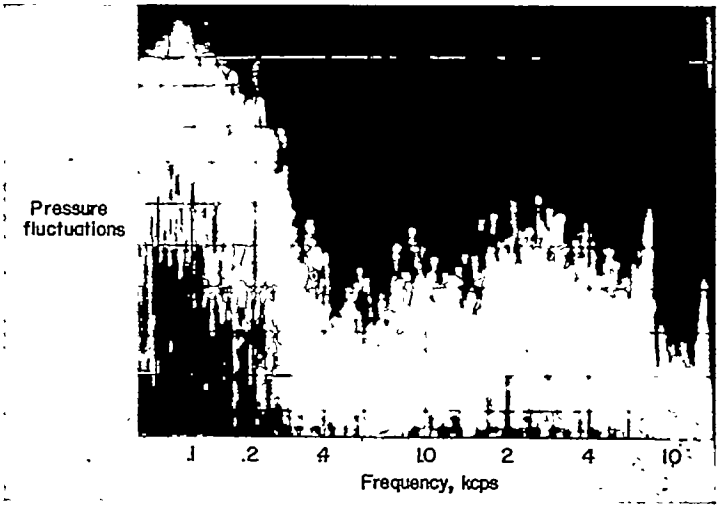

FIGURE 3.—Frequency spectrum of turbojet pressure fluctuations.

$\frac{x}{D}=15$; $\frac{d}{D}=2$.

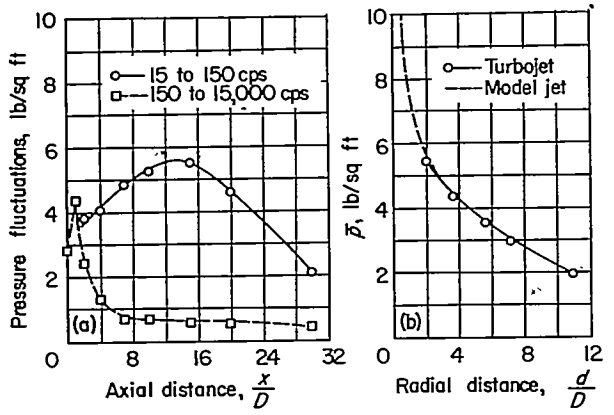

(a) Effect of axial distance. (b) Effect of radial distance.

$\frac{d}{D}$=2. $\frac{x}{D}$=15.

FIGURE 4.—Effects of distance on magnitude of pressure fluctuations of full-scale jet operating at rated thrust.

indicate that this maximum is largely due to a single high-pitched component of about 10,000 cps, which is presumably compressor or turbine whine. The more significant feature of the curve is that it clearly shows that the random pressure fluctuations in this frequency range are greatest near the nozzle and decrease rapidly with distance downstream.

On the other hand, the distribution of component pressure fluctuations in the frequency band from 15 to 150 cps indicates an increase with axial distance until a maximum pressure of about 5.5 lb/sq ft occurs at a point about 12 to 15 diameters downstream of the exit. Furthermore, the curve is comparatively flat, so that appreciable low-frequency content appears over a distance range of from approximately 2 to 20 diameters. In fact, comparison of the two curves of figure 4 (a) shows that at distances greater than about 2 diameters, the predominating pressure fluctuations are for frequencies lower than 150 cps.

From the practical standpoint, the effect of increasing radial distance on the magnitude of the fluctuations is of interest. Thus, the effects observed in a plane normal to the jet axis and located 15 diameters downstream (about at the maximum of the low-frequency curve) are shown in figure 4 (b) in the form of a radial pressure distribution. Since full-scale measurements were limited to a minimum distance of 2 diameters, some data from a 1-inch model jet having approximately the same temperature and velocity are included to indicate the probable trend at distances less than 2 diameters. The decrease of pressure with distance, as measured with the turbojet, is rather gradual. The model data, however, indicate that at distances less than 2 diameters from the boundary the curve becomes somewhat steeper. Even so, to obtain a 50-percent reduction in pressure requires an increase of radial distance from 0.5 to 3 diameters.

UNCHOKED OPERATION OF MODEL JETS

The scope of the full-scale measurements was somewhat limited by the test schedule of the airplane in which the engine was mounted; hence, it was deemed desirable to supplement the turbojet data with some results from a 1-inch model jet with heated air. The primary purpose of these model data, however, is to indicate general trends rather than to provide quantitative information.

Axial location of maximum pressure.—Figure 4 (a), which presents data taken along a line 2 diameters from the turbojet flow boundary, indicates that the magnitude of the pressure fluctuations is greatest at a point 12 to 15 diameters downstream of the nozzle. Results of model tests, however, indicate that the position of maximum pressure varies. It is dependent upon the radial distance at which the survey is made and upon the velocity of the jet. Figure 5 illustrates from model tests the nature of the variations produced by each of these parameters. In figure 5 (a) the distribution of pressure-fluctuation magnitude is plotted for four radial distances for a 1-inch jet operating at a temperature of 1,660° R and a velocity of 1,240 fps. As radial distance is increased, the point of maximum magnitude is seen to occur farther downstream. At a radial distance of 2 diameters (which is the same d/D as in figure 4 (a)), the maximum pressure occurs at 6 to 8 diameters downstream, or at roughly half the distance of the turbojet maximum. This difference is partly due to the velocity effect, which is illustrated in figure 5 (b). The curves apply to pressure distributions along the line $\frac{d}{D}$=2 at a constant jet temperature of 1,660° R but at various velocities from 600 fps to 1,870 fps. They indicate that velocity has a decided effect, which results in a shift of the maximum from 3 diameters to 10 diameters within the velocity range of the test. Even so, the curve for a velocity of 1,870 fps has a maximum at only 10 diameters, whereas the turbojet of figure 4 (a) indicated a maximum at 12 to 15 diameters at a slightly lower velocity.

The possibility arose that this discrepancy might have been due to ground effects, since the full-scale jet was only 3 diameters above ground whereas the model was some 70 diameters above it. Therefore, the model was operated at approximate turbojet values of temperature and Mach number and a survey was made by simulating the ground surface with a large sheet of plywood placed 3 diameters below the jet center line. Figure 6 presents a comparison of the pressure distributions obtained with the board and without it. Although these data are not sufficient to give a clear-cut indication that ground effects account for the discrepancy in distribution, the evidence is that the pressures far downstream are increased by much larger amounts

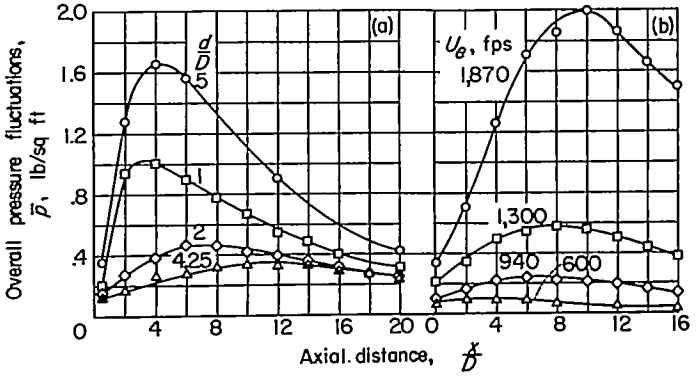

(a) Effect of radial distance. (b) Effect of jet velocity.

U_e=1,240 fps. $\frac{d}{D}$=2.

FIGURE 5.—Factors affecting the axial location of maximum pressure fluctuations from 1-inch model jet. T_e=1,660° R.

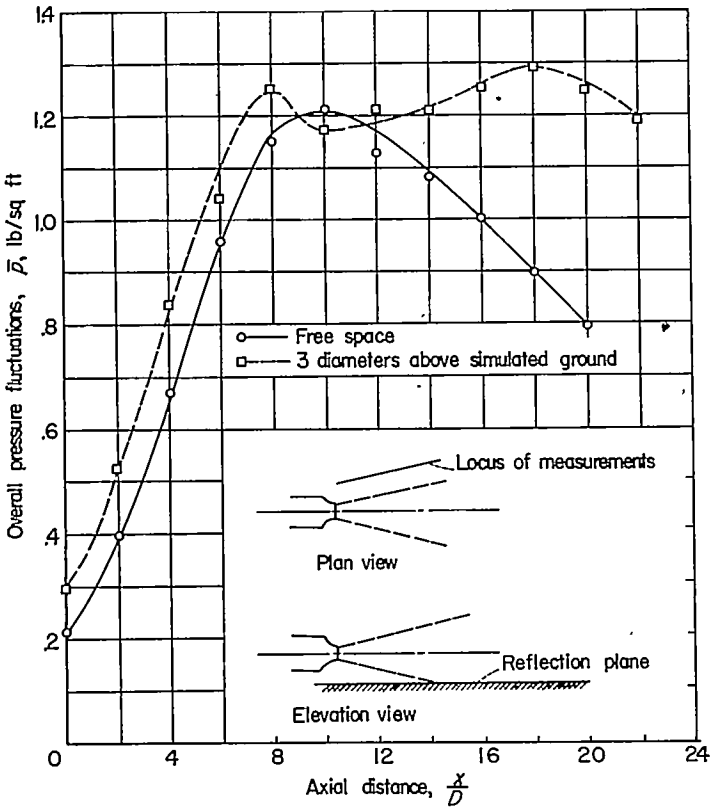

FIGURE 6.—Ground effect on pressure fluctuations. T_s=1,750° R; $\frac{d}{D}$=2; U_s=1,715 fps.

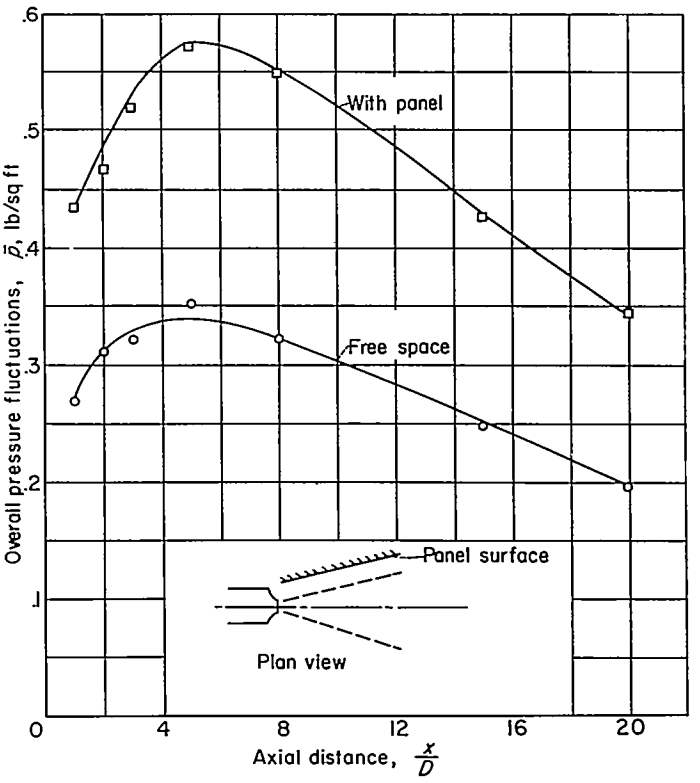

FIGURE 7.—Effect of panel on pressure fluctuations in 1-inch jet. $\frac{d}{D}$=1.5; U_s=700 fps.

than those near the nozzle. This result is probably due to the fact that, when the nozzle is situated only 3 diameters above ground, the flow, in spreading, impinges upon the ground in the vicinity of 8 diameters downstream. Thus, on the basis of these findings, it is believed that under free-space conditions the turbojet distributions would probably conform more nearly to those given in figure 5 for the model jet.

Effect of panel on pressures.—The effect which the presence of a wing or fuselage panel might have on the magnitude of pressure fluctuations is another factor which can be conveniently evaluated from model tests. For this test the 1-inch model jet was operated at 700 fps, without heat. Figure 7 illustrates the results obtained when a board simulating an aircraft panel was placed in the pressure field along a line 1.5 diameters from the jet boundary. Since the microphone diaphragm was mounted flush with the exposed board surface, the curves afford a comparison of panel surface pressure with free-space pressure. The results indicate that the presence of a panel in this orientation has a small effect on the axial station of maximum pressure and leads to higher pressure magnitudes at any given station. The pressures obtained with the panel as shown in figure 7 are roughly 50 percent to 80 percent higher than free-space pressures.

Effect of jet velocity.— As was shown in reference 1 for the far field, jet velocity is the most significant of the mean-flow parameters affecting overall pressure. In reference 1 the overall pressure in the far field of a low-turbulence jet was found to be related to velocity by a power law, the power being 3.0 to 3.7. By comparison, a power of 4.0 was obtained theoretically in reference 3. In the near field, however, this relationship of pressure to jet velocity is not necessarily expected to hold. Thus, figure 8 presents the results obtained from an experimental determination of the near-field relationship. Data were obtained during constant-temperature operation of a 1-inch jet over a convenient range of Mach numbers. Five stagnation-temperature conditions, ranging from 76° F (no heat) to 1,200° F, were used, and pressure measurements were made at various axial stations at a radial position 0.5 diameter from the jet boundary for each set of conditions. Data for two of these stations are shown in this figure. At 12 diameters downstream of the nozzle the data indicate a slope of about 2.2, whereas at 0.5 diameter downstream the slope is 1.4. At intermediate stations (not shown) a systematic variation of slope was observed. This result indicates that the pressure increases with velocity more rapidly at some distance downstream than at positions near the nozzle. This trend is consistent with the results shown in figure 5 (b), where the axial station of maximum pressure was shown to shift downstream with increasing jet velocity.

The present tests involved constant-temperature operation at variable Mach number and, since the same Mach numbers were used for each of several temperature conditions, overlapping velocity ranges result. However, as shown by figure 8, these various conditions yield pressure data which lie along a single curve. Thus, the implication is that the magnitude of pressure fluctuations in the near field can be appraised from knowledge of jet velocity alone, whether that parameter is varied by a change of nozzle pressure ratio or by a change of gas temperature, or both. Such an indication does not preclude the possibility that there are temperature, density, or Mach number effects, since any such effects are

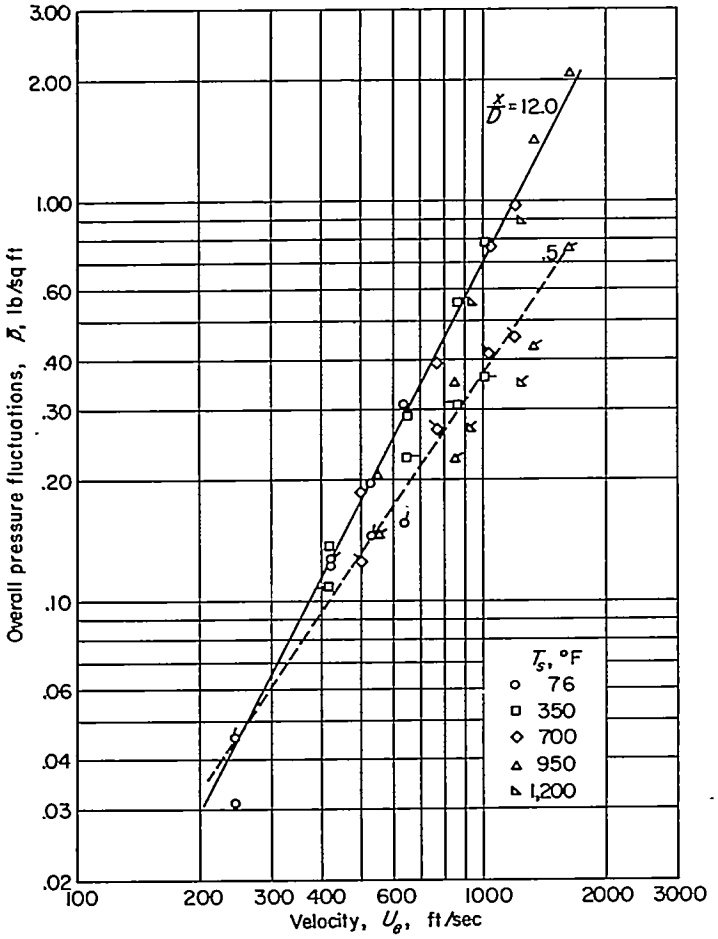

FIGURE 8.—Effect of jet velocity on overall magnitude of pressure fluctuations. $\frac{d}{D}$=0.5; D=1 inch. (Flagged symbols are for $\frac{x}{D}$=0.5.)

implicit in the data, but it does signify that together they produce only small net effect.

The slopes of the curves from the logarithmic plot of $\bar{p}$ against U_e in figure 8 differ from the value of 4.0 which occurs in the far field; hence, it follows that the slopes themselves are a function of radial distance. This effect is clearly illustrated by the curve of figure 9, in which the slopes of the logarithmic curves are plotted as a function of radial distance from the jet boundary at the nozzle. A rapid change of slope occurs at radial distances within the first few diameters from the boundary, and thereafter the slope change is at a lower rate.

CHOKED OPERATION OF MODEL JETS

Up to this point, the present report has dealt only with the nature of pressure fluctuations arising from subsonic (unchoked) jets. Overpressured (choked) operation, however, may also occur in a turbojet engine during thrust augmentation at take-off or in normal flight at high speed. Some engines may operate at slight overpressure even under static conditions with the engine operating at rated speed. Thus, an evaluation of the pressure fluctuations near the jet stream during choked operation is of interest. Because of the difficulties involved in full-scale measurements, however, data from small model jets are used to illustrate the nature of the fluctuations. These data were in all cases obtained with unheated air.

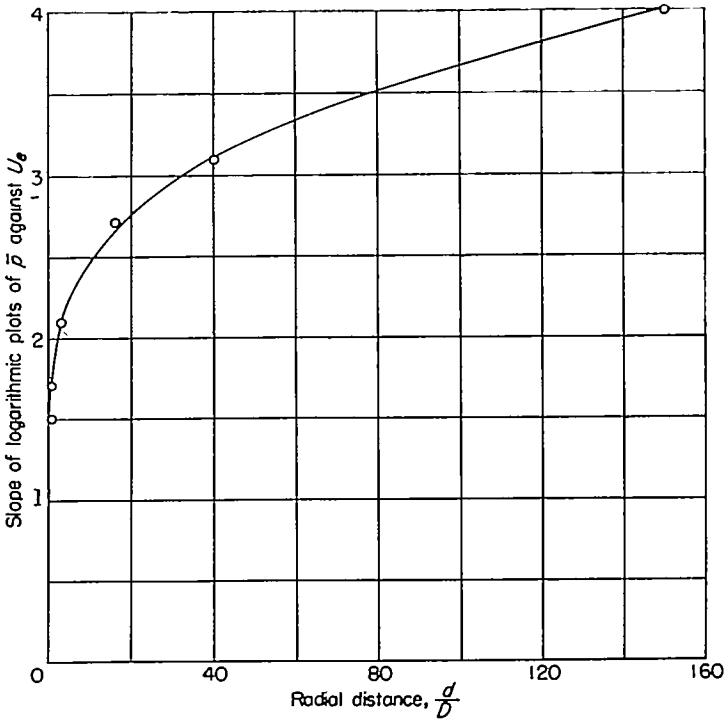

FIGURE 9.—Effect of radial distance on slope of overall-sound pressure curves. $\frac{x}{D}$=0.

Effect of choked operation on magnitude of pressure fluctuations.—The effect which overpressuring (choked operation), with its attendant shock formations, has on the magnitude of pressure fluctuations near the jet is of primary interest. Figure 10 illustrates the effects observed at a point 2.5 diameters downstream and 0.5 diameter from the boundary of a 1-inch jet as the nozzle pressure ratio is varied from low subsonic to large overpressure. The dashed vertical line represents the critical pressure ratio, or the boundary between choked and unchoked operation. The curve shows that the magnitude of pressure fluctuations increases rapidly up to a nozzle pressure ratio 3.67. At this point the magnitude is of the order of 20 times the value observed just before choking occurs. Further increase of nozzle ratio results in a sudden decrease of pressure fluctuations, followed eventually by another, more gradual increase beginning at a ratio of about 5. The shape of this curve and the magnitudes involved were found to apply to a 2-inch nozzle, as well as to the 1-inch nozzle, at the same geometrical location.

Frequency spectrum.—The large hump in the curve of figure 10 is associated with a rather sudden change in the frequency spectrum of the fluctuations. The nature of this change is illustrated in figure 11. The spectrum of figure 11 (a) is of the type generated when the nozzle pressure ratio is subcritical and the jet flow is entirely subsonic. It is very similar to the unchoked turbojet spectrum of figure 3 except that the frequencies involved are considerably higher because of the smaller diameter of the model jet. At a nozzle pressure ratio slightly above critical, however, a discrete-frequency component of very high intensity appears. Figure 11 (b) illustrates the spectrum under that condition. Although it is not evident in figure 11 because of the factor of 25 between the ordinate scales there, the discrete component occurs in addition to the random content. Its magnitude increases up

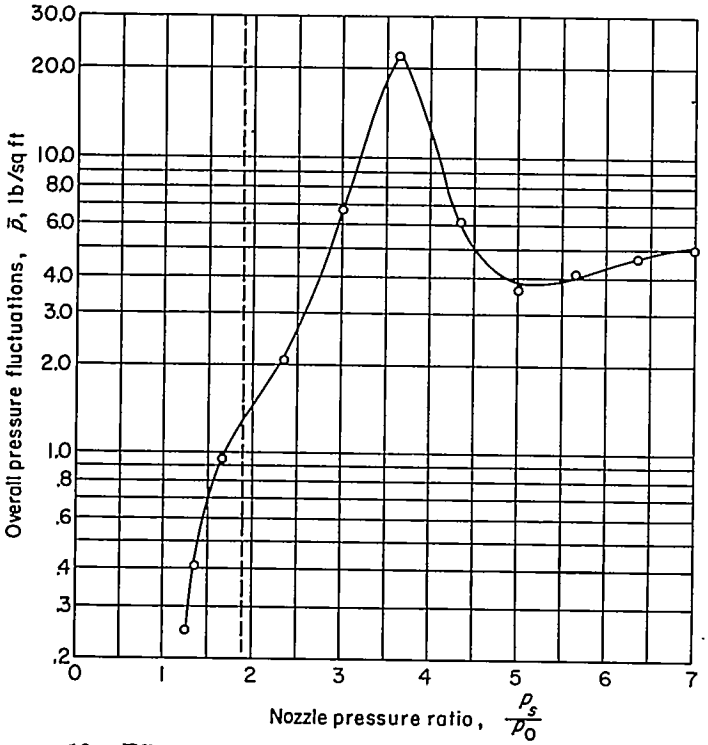

FIGURE 10.—Effect of nozzle pressure ratio on magnitude of pressure fluctuations. D=1 inch; $\frac{x}{D}$=2.5; $\frac{d}{D}$=0.5.

to a nozzle pressure ratio of 3.67. Thereafter, the magnitude diminishes with increasing pressure ratio until the component finally disappears from the spectrum at a nozzle pressure ratio of about 5. Thus, the hump in the overall-pressure-fluctuation curve of figure 10 is coincident with the presence of a discrete-frequency component.

This tendency for the choked jet to generate a discrete-frequency component was first reported in reference 6, which presented schlieren photographs of the flow and the sound field of a model configuration in which the periodicity was obvious.

The term "screech" is used hereinafter to denote this discrete-frequency component because it is particularly descriptive of the phenomenon as observed by the ear. This usage requires that a distinction be made between the present phenomenon, which is related to disturbances in the external flow, and another phenomenon involving a resonant condition inside the nozzle or tailpipe and also sometimes referred to as screech. The latter may occur in unchoked operation; whereas the former is exclusively a phenomenon of choked operation.

Flow studies of choked operation.—In an effort to obtain a better understanding of the mechanism of screech generation and to investigate the possibility of correlation between screech wavelength and, perhaps, shock spacing or stability, a series of shadowgraph studies of the flow during choked operation was made. Figure 12 presents sample shadowgraph records of the flow patterns existing in the flow from a 1-inch convergent nozzle at various nozzle pressure ratios in the choked range. Figures 12 (a) and 12 (b), at pressure ratios of 2.33 and 3.67, are associated with the onset of screech and the condition of maximum screech, respectively. Figures 12 (c) and 12 (d), at pressure ratios of 5.00 and 7.00, are associated with, respectively, the cessation of screech and the

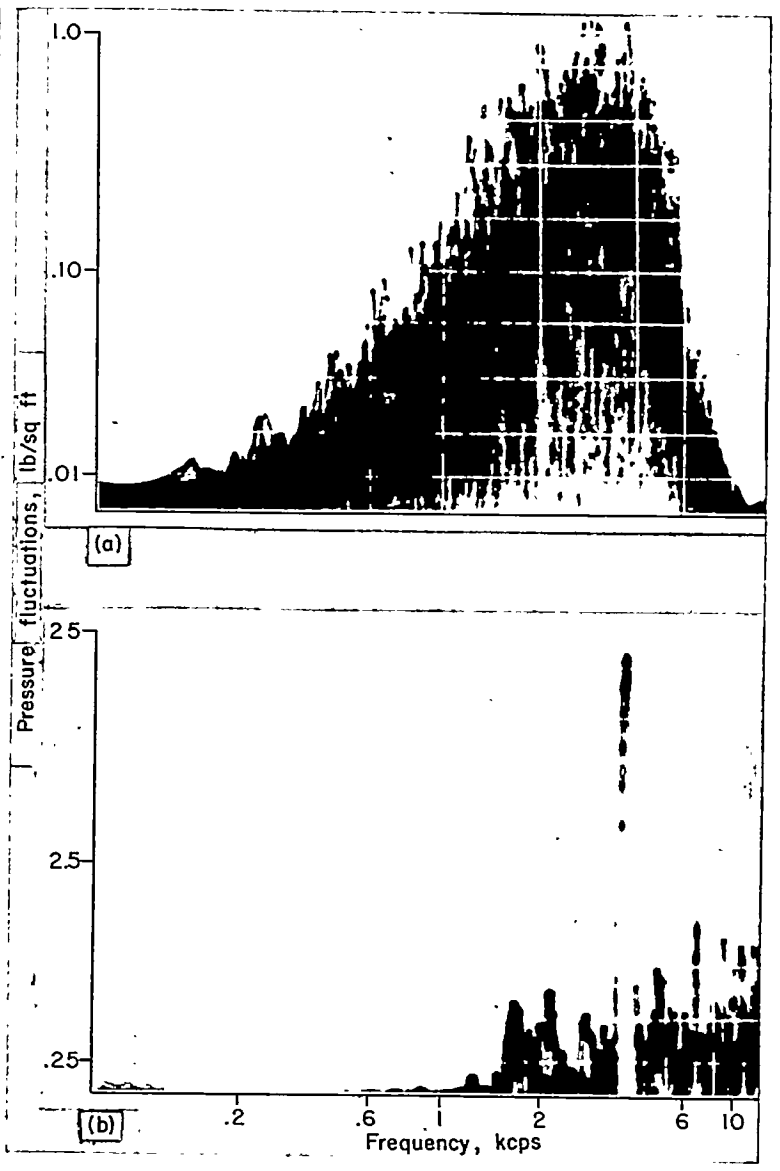

(a) Unchoked.
(b) Choked.

FIGURE 11.—Comparison of frequency spectrums of pressure fluctuations for unchoked and choked operation. D=1 inch; $\frac{x}{D}$=3; $\frac{d}{D}$=1.

limiting condition of the tests, where only random components are noticeable in the pressure spectrum.

In all of the records shown, a cellular shock pattern is evident, although the flow deceleration tends to become more nearly complete in a single shock at high pressure ratios. The spacing between the shocks increases with nozzle pressure ratio, as does the distance from the nozzle to the first shock. In figures 12 (a) and 12 (b), both associated with the screech condition, flow disturbances suggestive of partly formed toroidal vortices are apparent in the vicinity of the shock formations. These disturbances appear to be of the same form as those observed by schlieren methods in references 6 and 7. At the lowest pressure ratio these patterns are symmetrical about the jet, but at a pressure ratio of 3.67 they appear alternately on opposite sides of the jet, along its length. Since no such formations are evident in figures 12 (c) and 12 (d), where screech is not present, there is reason to believe that these flow disturbances are associated with generation of the screech component.

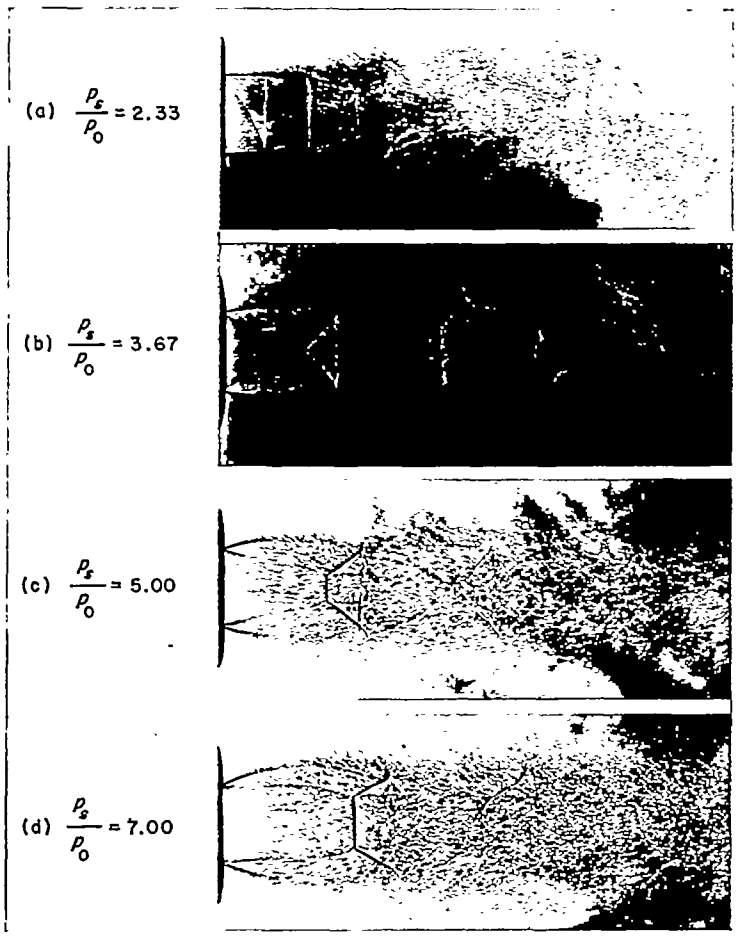

FIGURE 12.—Flow patterns of 1-inch choked jet.

Screech-frequency studies.—Some studies were made to determine the relation that existed between the shock spacing and the wavelength of screech. The results obtained with a 1-inch orifice (chosen because of its more even frequency variation as compared with a nozzle) are given in figure 13. In figure 13 (a), dimensionless screech wavelength and distance between shocks are plotted as functions of nozzle pressure ratio. The shock distances were measured between first and second shocks at their radial extremities. The resultant curves indicate a steady widening of the distance between shocks and a concurrent lengthening of the screech wavelength. Reference 6 showed that in two-dimensional jets the two variations are of the same form. In the present tests, however, with a three-dimensional jet, the variations

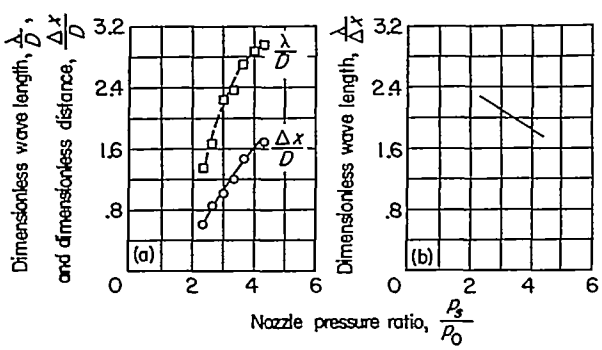

(a) Screech wavelength and shock-distance variations.

(b) Relation between shock distance and screech wavelength.

FIGURE 13.—Variation of shock distance and screech wavelength for 1-inch orifice.

are seen to be somewhat dissimilar. A plot of $\lambda/\Delta x$, as given in figure 13 (b), gives decreasing values as nozzle pressure ratio is increased; whereas observations of reference 6 with a two-dimensional jet result in a constant ratio of wavelength to shock distance.

Scale effect on screech frequency.—In the course of these tests the screech phenomenon was observed to occur with orifices of 0.275-inch, 0.500-inch, and 1.00-inch diameters and with nozzles of 1.00-inch and 2.00-inch diameters. Figure 14 illustrates the variation of screech frequency with pressure ratio observed with each configuration. These curves indicate that although there are dissimilarities among the various curves, particularly between results obtained with a nozzle and with an orifice, the screech frequency at a given pressure ratio is roughly proportional to the inverse of the nozzle diameter. A point of interest in this figure is the difference in shape between the curve for the 1-inch nozzle and that for the 1-inch orifice. Both appear to approach a common value at the upper end of the pressure range, but the nozzle curve tends to flatten at lower pressure ratios than the orifice curve.

Axial pressure distribution.—It should not be inferred from the choice of distance, that is, between first and second shocks, for figure 13 (a) that only in that region is the screech component apparent. On the contrary, pressure distributions along a 15° line near the jet indicate a series of maximums and minimums during screech. For example, figure 15 gives the distribution along a line 0.1 diameter from the subsonic boundary of sharp-edged-orifice flow at a pressure ratio of 3.67, which corresponds to a very pronounced screech condition. For comparison the distribution at a

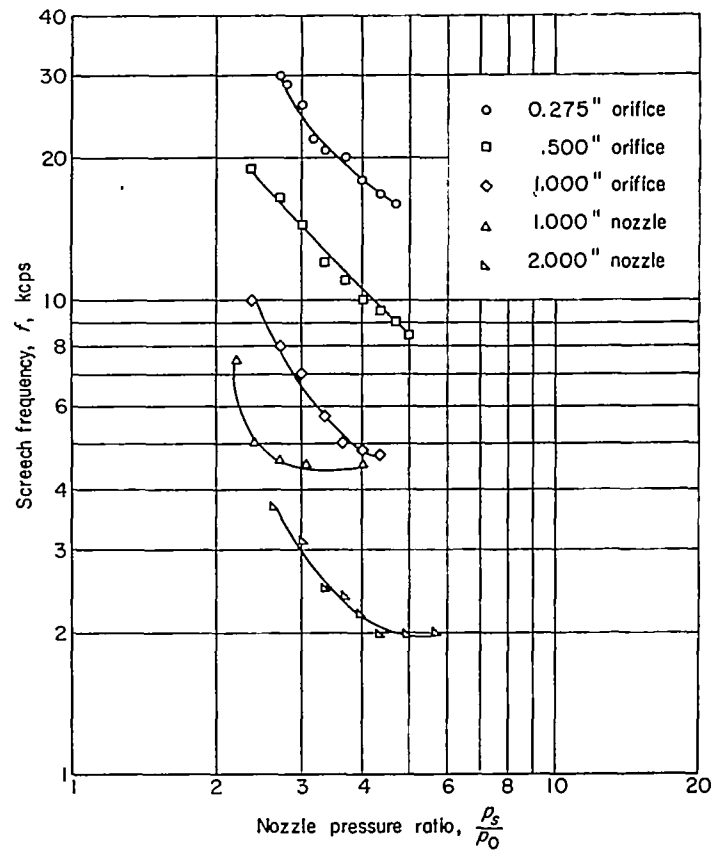

FIGURE 14.—Effect of jet diameter on screech frequency.

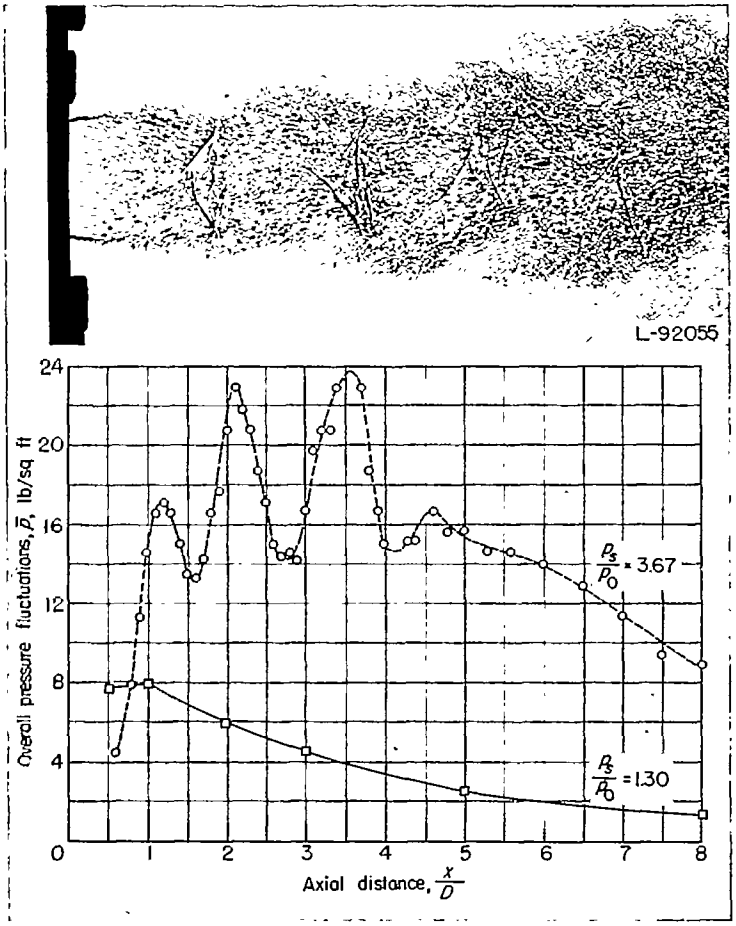

FIGURE 15.—Axial distributions of magnitude of pressure fluctuations. D=1 inch; $\frac{d}{D} \approx 0.1$.

subsonic pressure ratio of 1.30 is given also. The dashed curve, associated with the screech condition, indicates four maximums and therefore implies that the screech component may have at least four sources for this condition. Comparison of the curve with the shadowgraph record shows that the maximums lie at points slightly downstream of the shock formations. The shadowgraph record also indicates the presence in the flow of disturbances of the type shown in figure 12 (b) for nozzle flow.

Shock-motion studies.—Since the screech maximums lie near the shock formations and since the flow disturbances are observed also in the vicinity of the shocks, an investigation of the stability of the shocks during the screech condition appeared appropriate. A sample result of such a study, made with the apparatus of figure 2 (b) for a 2-inch nozzle, is shown in figure 16. Figure 16 compares the waveform of pressure fluctuations and the shock-motion waveform during screech. The results presented were not obtained simultaneously and therefore phase comparisons cannot be made. A segment of the first shock near its radial extremity was selected for observation. The pressure trace indicates that the waveform is essentially a sinusoid with smaller random components superimposed. The shock-motion waveform, on the other hand, is rather irregular, but a cyclic tendency is evident. The frequency is roughly the same as the screech frequency, about 2,000 cps. Similar records obtained in the range where only random pressure fluctuations exist do not exhibit this periodic behavior; therefore, it appears that the screech condition is definitely associated with an oscillatory motion of the shock formation.

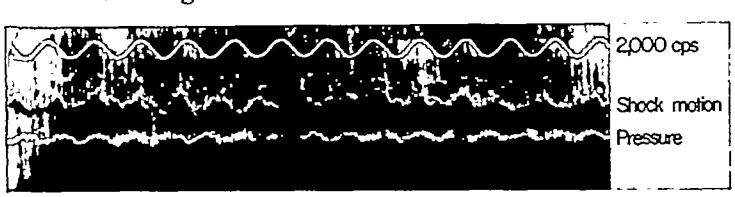

FIGURE 16.—Comparison of pressure waveform and shock-motion waveform during screech. D=2 inches; $\frac{P_s}{P_0}$=3.67.

Screech in hot jets.—Although the data thus far presented for the choked operating condition apply directly to cold-air jets, some tests with a model burner have established the existence of the screech phenomenon at high temperatures as well. These exploratory tests with heated air, however, have indicated that the magnitude of the screech component relative to the random components is much lower at high temperatures than at low temperatures.

SOME DEVICES FOR NOISE REDUCTION

REDUCTION OF PRESSURE FLUCTUATIONS FROM UNCHOKED JETS

In the course of the model tests with unchoked nozzles, it was found that the frequency spectrums could be changed and some reduction of pressure magnitudes could be obtained by inserting a single sheet of wire screen into the flow and normal to the flow axis. Since this scheme might have application in the design of ground mufflers for jets, some sample results are given herein.

The frequency spectrum of the far-field noise was found to be affected greatly by the presence of the screen and, for a given jet diameter and velocity, the effects varied with screen axial position and screen mesh size. For example, figure 17 illustrates some results obtained when an 8-mesh screen of 0.023-inch wire diameter was placed in a 0.75-inch jet operating at 900 fps. The data were obtained at a point in the far sound field 64 diameters from the nozzle and at an azimuth angle of 140°. The figure compares the free-jet spectrum with the spectrums obtained when the screen was located at distances of ⅛ diameter and 2 diameters downstream of the nozzle. Comparison of the spectrum of figure 17 (b) with the free-jet spectrum of figure 17 (a) indicates that the presence of the screen ⅛ diameter from the nozzle has reduced the noise to a considerable extent, the lower-frequency components being reduced more than the higher-frequency ones.

The spectrum of figure 17 (c) was obtained with the screen 2 diameters from the nozzle. It is seen to contain several high-intensity discrete components which are believed to be of edge-tone origin, and the overall pressure level is only slightly lower than that of the free jet. Even so, the random components have been appreciably reduced. It is conceivable that, from a sound-treating standpoint, the spectrum of figure 17 (c) might still be simpler to cope with than that of figure 17 (a), because the energy appears at somewhat higher frequencies.

The effects on overall sound pressure which accompany these spectrum changes are illustrated in figure 18 for the 0.75-inch jet. Overall sound pressures, as observed at an angle of 140° and a distance of 64 diameters, are plotted as a function of screen position in inches downstream of the

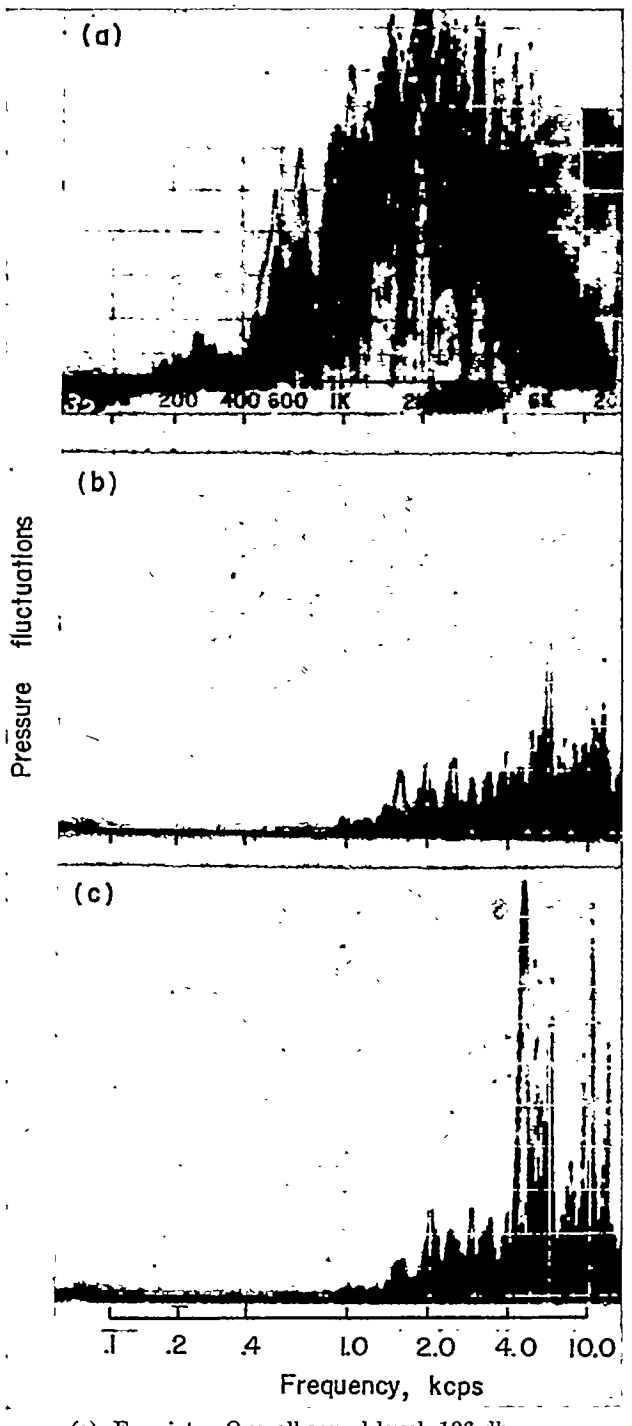

(a) Free jet. Overall sound level, 106 db.
(b) Screen at $D/3$. Overall sound level, 95 db.
(c) Screen at $2D$. Overall sound level, 105 db.

FIGURE 17.—Effect of screen on spectrum of 0.75-inch jet (logarithmic ordinate). 8-mesh screen; 0.023-inch wire; U_e=900 fps; ψ=140°; $\frac{z}{D}$=64.

nozzle. The pressure measured with no screen in the flow is given by the horizontal line at 0.077 pound per square foot. Comparisons of this pressure with that measured for various screen positions show that overall sound pressure is reduced for all screen positions up to 2.3 inches (about 3 diameters) downstream.

In order to investigate the effect of a device of this sort on the angular distribution of overall sound pressure, a grid of water-cooled tubes was used with a 1-inch heated jet. The

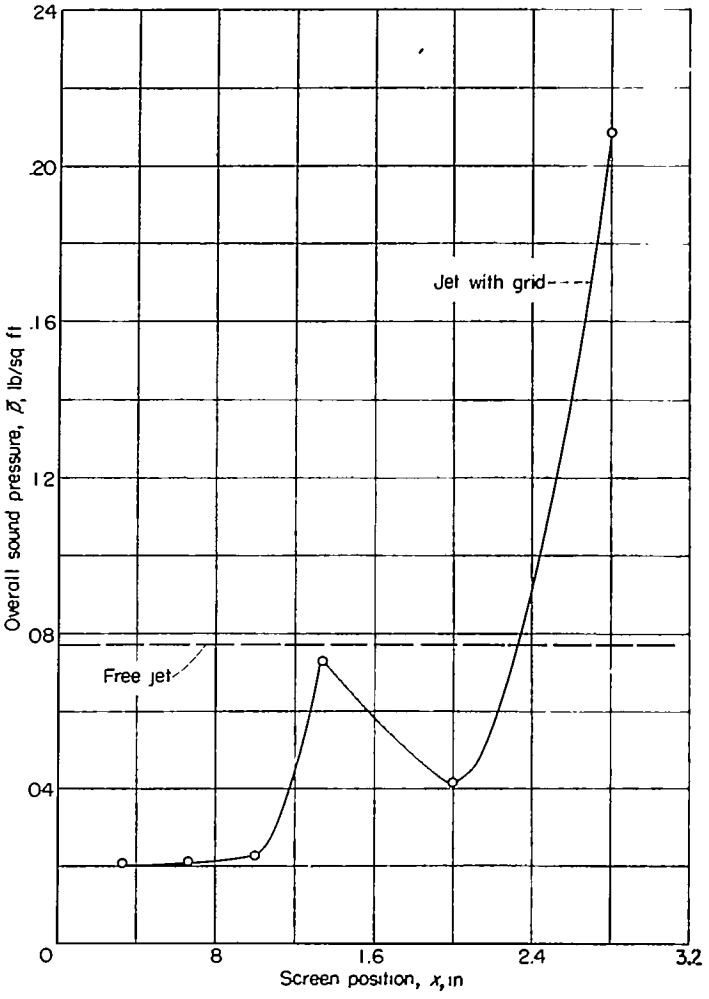

FIGURE 18.—Effect of screen on overall sound pressure from 0.75-inch jet. 8-mesh screen; 0.023-inch wire; U_e=900 fps; ψ=140°; $\frac{z}{D}$=64.

grid consisted of tubes, ⅛-inch in outside diameter, through which water was passed for cooling purposes. The jet was operated at a stagnation temperature of 1,400° F and a velocity just below sonic. Figure 19 presents a comparison of the overall pressure distributions for the free jet and the jet with grid at a distance of 150 nozzle diameters from the center point of the nozzle. The indications are that the grid is effective in reducing overall sound pressure at all azimuth angles greater than 90°. The greatest reduction observed is of the order of 10 to 12 decibels and occurs along the azimuth which in the free jet gives highest pressures.

The beneficial effect of the screens appears to result from the deceleration of the flow to considerably lower velocities at a point upstream of the region of greatest noise generation. Consequently, the reduction is greatest at the lower frequencies, since noise at these frequencies has been shown to originate principally in the region downstream of about 2 diameters. In the course of the present tests, screens of various mesh sizes were investigated and, in general, the results indicated that the sound reductions increased as the mesh size was made smaller; however, the back pressure in the nozzle due to the presence of smaller-mesh screens also increases. For the 8-mesh screen located ⅛ diameter from the nozzle exit the back pressure was 0.2 inch of mercury at a jet exit velocity of 900 fps.

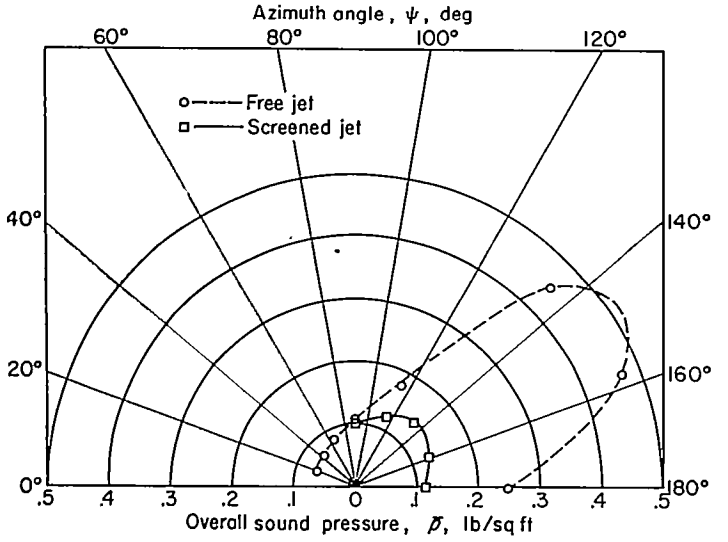

FIGURE 19.—Effect of a grid on the overall noise from a high-temperature model jet. D=1 inch; $\frac{z}{D}$=150; T_s=1,400° F.

SCREECH ELIMINATION IN CHOKED JETS

In references 4 and 6 several methods of obtaining reduction in the magnitude of pressure fluctuations from a choked jet were discussed. Among these were such devices as a toothed nozzle and a gauze-cylinder extension to the nozzle to allow shock-free expansion of the supersonic flow. Several exploratory methods of a similar nature were investigated during the present tests. One such method, not previously reported, proved very effective in reducing the magnitude of the screech component. This method involved the use of small auxiliary orifices to introduce turbulence into the main stream at a point just downstream of the main jet exit. (See sketch in fig. 20.) The configuration consisted of a 1-inch knife-edge orifice with four 1/32-inch holes drilled through the beveled face, whereby a small auxiliary supply of air from the settling chamber was allowed to enter the main flow at an angle of about 45°.

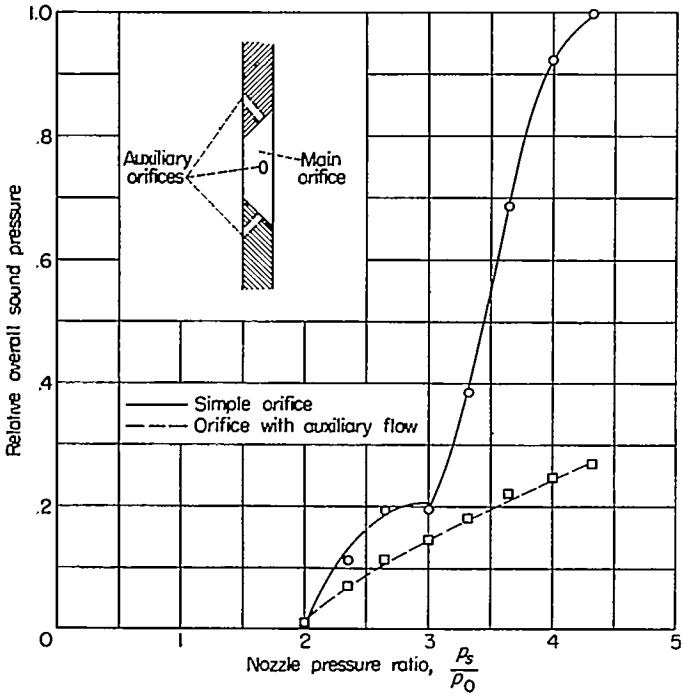

FIGURE 20.—Effect of auxiliary orifices on relative overall pressure-fluctuation magnitude. D=1 inch; D_a=0.031 inch.

An illustration of the reduction in magnitude of the overall pressure fluctuations obtained by this method is shown in figure 20, which compares on a relative pressure basis the data obtained at a point just outside the jet boundary and approximately 3 diameters downstream. Any scheme which reduces the discrete frequency noise components will essentially eliminate the peaks in the axial pressure distribution curve of figure 15. The reductions obtained are a function of the relative contributions of the discrete component and the random components and, hence, are much greater at some field points than at others. This same result applies to locations in the far field where the amount of noise reduction is a function of the azimuth angle. The net result of eliminating the screech component appears to be a decrease of the total radiated acoustical energy. In one test configuration where screeching was severe, some noise reduction was obtained at all azimuth angles and this reduction resulted in a decrease of 3 decibels in the total radiated energy.

Shadowgraph records show that this decrease is coincident with elimination of the vortex flow patterns associated with screech. Figure 21 illustrates the change in the flow pattern when auxiliary orifices are used at the highest pressure ratio of the tests. The top record was obtained with the auxiliary orifices plugged. Screech was present and the vortex formations are evident. The lower record was obtained at the same pressure ratio with the auxiliary orifices in operation. The screech component was virtually eliminated and the flow disturbances are shown to be greatly reduced. Thus, the generation of screech is again indicated to be associated with formation of the vortex-like disturbances.

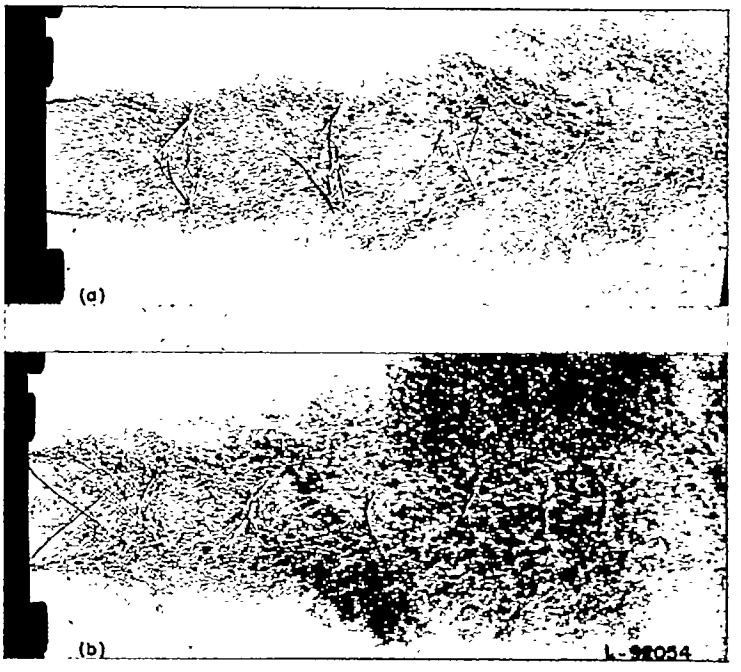

(a) No auxiliary orifices (screeching).
(b) With auxiliary orifices.

FIGURE 21.—Effect of auxiliary orifices on flow of choked jet. $\frac{p_s}{p_0}$=3.67; D=1 inch; D_a=0.031 inch.

CONCLUSIONS

Results have been presented from an investigation of the near sound-pressure field of a full-scale unchoked turbojet and of both choked and unchoked model jets.

The near-field investigation of pressure fluctuations from the full-scale turbojet engine indicates the following conclusions:

1. The fluctuations are random and the largest components occur within a fairly narrow band at frequencies less than 150 cps.

2. Along a line 2 nozzle diameters from the jet boundary, maximum pressure fluctuations occur at about 12 to 15 diameters downstream of the nozzle.

Results obtained with unchoked model jets indicate:

1. The position of maximum pressure magnitude along a line parallel to the jet boundary is a function of jet velocity and the radial distance of the survey.

2. Pressure magnitude is about 50 percent to 80 percent higher at a panel surface than in free space when the panel is oriented parallel to the jet boundary.

3. The overall magnitude of pressure fluctuations varies with jet velocity to about the second power near the jet, whether the velocity increase is effected at constant Mach number with variable temperature or at constant temperature with variable Mach number.

4. The exponent of the power function relating overall sound pressure and jet velocity increases systematically with radial distance from the nozzle.

5. The use of a wire screen in the jet flow at points a diameter or so downstream of the nozzle reduces the low-frequency components of the random noise spectrum by a considerable amount. Overall sound pressures at azimuth angles greater than 90° are thus lowered, primarily as a result of the large decreases in the lower-frequency components.

Results obtained with choked model jets indicate:

1. A high-intensity, discrete-frequency component occurs during a part of the choked operating range. This component is associated with the presence of flow disturbances of toroidal-vortex form and with oscillation of the shock formations.

2. For a given nozzle size, the frequency of the screech component bears some relation to the shock spacing. Frequency is roughly proportional to the inverse of the nozzle diameter.

3. The use of four small auxiliary orifices to introduce turbulence into the main stream just downstream of the exit reduced the magnitude of the screech component by a considerable amount.

LANGLEY AERONAUTICAL LABORATORY,
NATIONAL ADVISORY COMMITTEE FOR AERONAUTICS,
LANGLEY FIELD, VA., *February 19, 1954.*

REFERENCES

1. Lassiter, Leslie W., and Hubbard, Harvey H.: Experimental Studies of Noise From Subsonic Jets in Still Air. NACA TN 2757, 1952.
2. Von Gierke, H. E., Parrack, H. O., Gannon, W. J., and Hansen, R. G.: The Noise Field of a Turbo-Jet Engine. Jour. Acous. Soc. Am., vol. 24, no. 2, Mar. 1952, pp. 169–174.
3. Lighthill, M. J.: On Sound Generated Aerodynamically. I. General Theory. Proc. Roy. Soc. (London), ser. A, vol. 211, no. 1107, Mar. 20, 1952, pp. 564–587.
4. Westley, R., and Lilley, G. M.: An Investigation of the Noise Field From a Small Jet and Methods for Its Reduction. Rep. No. 53, College of Aero.; Cranfield (British), Jan. 1952.
5. Melton, Ben S., Prescott, Rochelle, and Gayhart, Everett L.: A Working Manual for Spark Shadowgraph Photography. Bumblebee Rep. No. 90 (Bur. Ord., U. S. Navy Contract No. NOrd 7386), The Johns Hopkins Univ., Appl. Phys. Lab., Dec. 1948.
6. Powell, Alan: A "Schlieren" Study of Small Scale Air Jets and Some Noise Measurements on Two-Inch Diameter Air Jets. Rep. No. NC 136, Univ. College, Southampton (British), Dec. 1951.
7. Powell, Alan: The Noise of Choked Jets. Jour. Acous. Soc. Am., vol. 25, no. 3, May 1953, pp. 385–389.